一般社団法人　電子情報通信学会
THE INSTITUTE OF ELECTRONICS,
INFORMATION AND COMMUNICATION ENGINEERS

信学技報
IEICE Technical Report
RCS2015-261(2015-12)

Frequency-Domain Blind Selected Mapping Technique for Space-Time Block Coded Low-PAPR SC-FDE

Amnart Boonkajay † and Fumiyuki Adachi ‡

† ‡ Department of Communications Engineering, Graduate School of Engineering, Tohoku University
6-6-05 Aza-Aoba, Aramaki, Aoba-ku, Sendai, Miyagi, 980-8579 Japan
E-mail: † amnart@mobile.ecei.tohoku.ac.jp ‡ adachi@ecei.tohoku.ac.jp

Abstract Single-carrier with frequency-domain equalization (SC-FDE) is a promising transmission technique obtaining frequency diversity gain with low peak-to-average power ratio (PAPR) property of transmit signal. PAPR of SC-FDE signal increases when transmit filtering or high-level modulation is applied. We have recently proposed a blind frequency-domain selected mapping (FD-SLM) technique, which phase-rotates each subcarrier component of SC signal to be transmitted at a transmitter and performs joint blind phase rotation pattern estimation and data detection at a receiver. The blind FD-SLM requires no side-information sharing and hence, does not cause any spectrum efficiency (SE) degradation. In this paper, we extend the blind FD-SLM technique to space-time block coded SC-FDE (STBC-SC-FDE). A common phase rotation pattern is selected so as to minimize the maximum value of PAPR among all transmit signals from user terminal antennas after STBC encoding. Performance evaluation of STBC-SC-FDE with the proposed blind FD-SLM is done by computer simulation in aspects of PAPR and bit-error rate (BER). It is confirmed that the PAPR can be reduced without significant degradation of BER performance and without side-information sharing.

Keyword Space-time block coding (STBC), Single-carrier (SC) transmission, peak-to-average power ratio (PAPR), selective mapping (SLM), frequency-domain equalization (FDE)

1. Introduction

Small-cell network using distributed antennas [1] is a promising candidate for the fifth-generation (5G) mobile communications as it can simultaneously achieve high spectrum efficiency (SE) and energy efficiency (EE). Single-carrier (SC) transmission with frequency-domain equalization (FDE) [2] is very attractive for uplink transmission since it is robust against frequency-selective fading [3], while its waveform has low peak-to-average power ratio (PAPR) property [4]. The PAPR of SC-FDE transmit signal, however, becomes higher when higher modulation level is used [5]. Therefore, PAPR reduction is still an important issue for 5G uplink transmission although small-cell architecture can reduce the average transmit power owing to shorter range of transmission.

A PAPR reduction technique based on phase rotation called selected mapping (SLM) [6] has been extensively studied for orthogonal frequency division multiplexing (OFDM) transmission. SLM is known as a promising technique providing effective PAPR reduction without signal distortion but with small overhead bits. Recently, we proposed [7] an SLM for SC-FDE (or discrete Fourier transform (DFT)-precoded OFDM) transmission, called frequency-domain SLM (FD-SLM). FD-SLM applies phase rotation to each subcarrier. We also proposed a maximum-likelihood based joint blind phase rotation pattern estimation and data detection [8] which requires no transmission of side-information.

Multi-input multi-output (MIMO) transmission has been attracting much attention for improving SE through either spatial diversity gain or spatial multiplexing [9]. A frequency-domain space-time block coded (STBC) diversity [10, 11] can obtain frequency diversity gain as well as spatial diversity gain. It should be noticed that there still exists the problem of high-PAPR signal when either the transmit filtering or higher-level data modulation is applied similar to the single-antenna SC-FDE case. However, the existing PAPR reduction techniques for SC-FDE, including FD-SLM proposed in [7-8], was discussed only in the case of single-antenna transmission.

Motivated by the above discussions, we propose a PAPR reduction technique for STBC-SC-FDE transmission in this paper based on a modification of FD-SLM. Since the SLM needs to consider the output waveforms from all transmit antennas, a common phase rotation pattern is selected and multiplied in order to minimize the maximum value of PAPR among all transmit signals from user terminal antennas. The reason for using the common phase rotation pattern instead of applying individual phase rotation pattern for each antenna is to preserve the STBC code orthogonality and allows the ML-based blind phase rotation pattern estimation and data detection. PAPR and bit-error rate (BER) performances of STBC-SC-FDE using the proposed blind FD-SLM are evaluated by computer simulation. It is confirmed that the PAPR of STBC-SC-FDE signal can be reduced with no side-information sharing and no significant BER degradation.

Table 1 Relationship of N_t, J, Q and STBC coding rate.

N_t	J	Q	$R_{\mathrm{STBC}}=J/Q$
1	1	1	1
2	2	2	1
3	3	4	3/4
4	3	4	3/4

2. STBC-SC-FDE transmitter with FD-SLM

STBC-SC-FDE transmitter with FD-SLM is illustrated by Fig. 1. For simplicity, point-to-point transmission is assumed in this paper, i.e. path-loss and shadowing-loss are neglected for all user equipment-received distributed antenna links (assuming uplink transmission).

2.1. Transmitter

We begin with J blocks of N_c-length data-modulated transmit vector $\mathbf{d}_j=[d_j(0),d_j(1),\ldots,d_j(N_c-1)]^T$, $j=0\sim J-1$. $\mathbf{d}_j$ is transformed into frequency domain by N_c-point DFT, yielding $\mathbf{D}_j=\mathbf{F}_{N_c}\mathbf{d}_j$ where $\mathbf{F}_{N_c}$ is is expressed by

$$\mathbf{F}_{N_c}=\frac{1}{\sqrt{N_c}}\begin{bmatrix}1 & 1 & \cdots & 1\\ 1 & e^{\frac{-j2\pi(1)(1)}{N_c}} & \cdots & e^{\frac{-j2\pi(1)(N_c-1)}{N_c}}\\ \vdots & \vdots & \ddots & \vdots\\ 1 & e^{\frac{-j2\pi(N_c-1)(1)}{N_c}} & \cdots & e^{\frac{-j2\pi(N_c-1)(N_c-1)}{N_c}}\end{bmatrix}, \quad (1)$$

and its Hermitian transpose $\mathbf{F}_{N_c}^H$ represents inverse DFT (IDFT) operation.

After that, J blocks of frequency-domain components $\mathbf{D}_j$ are encoded by STBC encoding [10] into N_t parallel streams of Q encoded blocks $\mathbf{S}_{N_t}=[\mathbf{S}_0,\ldots,\mathbf{S}_q,\ldots,\mathbf{S}_{Q-1}]$ where $\mathbf{S}_q=[\mathbf{S}_{q,0},\ldots,\mathbf{S}_{q,n_t},\ldots,\mathbf{S}_{q,N_t-1}]^T$. The STBC-encoded blocks $\mathbf{S}_{N_t}$ depend on the number of transmit antennas N_t and is expressed by [12]

$$\mathbf{S}_{N_t=1}=\mathbf{D}_0, \quad (2a)$$

$$\mathbf{S}_{N_t=2}=\frac{1}{\sqrt{2}}\begin{bmatrix}\mathbf{D}_0 & -\mathbf{D}_1^*\\ \mathbf{D}_1 & \mathbf{D}_0^*\end{bmatrix}, \quad (2b)$$

$$\mathbf{S}_{N_t=3}=\frac{1}{\sqrt{3}}\begin{bmatrix}\mathbf{D}_0 & -\mathbf{D}_1^* & -\mathbf{D}_2^* & \mathbf{0}\\ \mathbf{D}_1 & \mathbf{D}_0^* & \mathbf{0} & -\mathbf{D}_2^*\\ \mathbf{D}_2 & \mathbf{0} & \mathbf{D}_0^* & \mathbf{D}_1^*\end{bmatrix}, \quad (2c)$$

$$\mathbf{S}_{N_t=4}=\frac{1}{\sqrt{4}}\begin{bmatrix}\mathbf{D}_0 & -\mathbf{D}_1^* & -\mathbf{D}_2^* & \mathbf{0}\\ \mathbf{D}_1 & \mathbf{D}_0^* & \mathbf{0} & -\mathbf{D}_2^*\\ \mathbf{D}_2 & \mathbf{0} & \mathbf{D}_0^* & \mathbf{D}_1^*\\ \mathbf{0} & \mathbf{D}_2 & -\mathbf{D}_1 & \mathbf{D}_0\end{bmatrix}. \quad (2d)$$

In addition, the relationship between J and Q, and the corresponding coding rate $R_{\mathrm{STBC}}=J/Q$, is shown in Table 1. It is observed that there is no SE degradation when $N_t=2$.

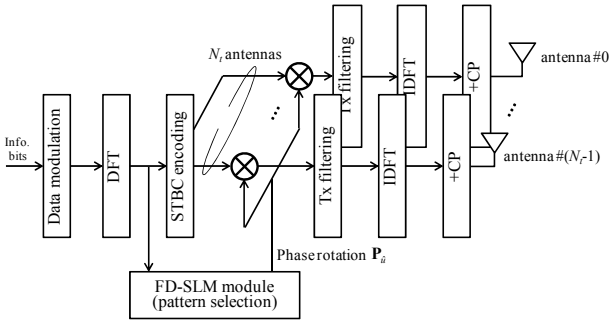

Fig.1 STBC-SC-FDE transmitter with FD-SLM.

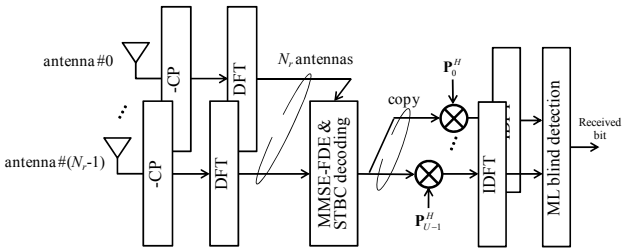

Fig.2 STBC-SC-FDE receiver with joint blind phase rotation pattern estimation and data detection.

A phase rotation matrix $\mathbf{P}_{\hat{u}}=diag[P_{\hat{u}}(0),\ldots,P_{\hat{u}}(N_c-1)]$ which its diagonal line contains common phase rotation pattern, following by the transmit filtering matrix $\mathbf{H}_T=diag[H_T(0),\ldots,H_T(N_c-1)]$, are multiplied to all STBC transmit blocks in frequency domain. The transmit filtering is assumed to be square-root raised cosine (SRRC) filtering with roll-off factor α=0. The selection criterion for phase rotation pattern $\mathbf{P}_{\hat{u}}$ is described in details in Subsection 2.2. After that, the phase-rotated q-th block of frequency spectrum to be transmitted at the n_t-th antenna $\widetilde{\mathbf{S}}_{\hat{u},q,n_t}$ can be expressed by

$$\widetilde{\mathbf{S}}_{\hat{u},q,n_t}=\mathbf{H}_T\mathbf{P}_{\hat{u}}\mathbf{S}_{q,n_t}. \quad (3)$$

In case of N_t=2, $\widetilde{\mathbf{S}}_{\hat{u},q,n_t}$ is expressed by

$$\widetilde{\mathbf{S}}_{\hat{u},N_t=2}=\frac{1}{\sqrt{2}}\begin{bmatrix}\mathbf{H}_T\mathbf{P}_{\hat{u}}\mathbf{D}_0 & -\mathbf{H}_T\mathbf{P}_{\hat{u}}\mathbf{D}_1^*\\ \mathbf{H}_T\mathbf{P}_{\hat{u}}\mathbf{D}_1 & \mathbf{H}_T\mathbf{P}_{\hat{u}}\mathbf{D}_0^*\end{bmatrix}. \quad (4)$$

After that, $\widetilde{\mathbf{S}}_{\hat{u},q,n_t}$ is transformed back into time domain by N_c-point IDFT, yielding the q-th time-domain transmit block to be transmitted at the n_t-th antenna $\widetilde{\mathbf{s}}_{\hat{u},q,n_t}=\mathbf{F}_{N_c}^H\widetilde{\mathbf{S}}_{\hat{u},q,n_t}$. Finally, the last N_g samples of transmit block are copied as a cyclic prefix (CP) and inserted into the guard interval (GI), then a CP-inserted signal block of N_g+N_c samples is transmitted. We also would like to mention that there is no requirement for side-information sharing between transceiver.

2.2. FD-SLM algorithm

Assuming that an N_c-length time-domain transmit block is represented by $\mathbf{s}=[s(0),s(1),\ldots,s(N_c-1)]^T$, PAPR is calculated over an oversampled block, which is

$$\mathrm{PAPR}(\mathbf{s}) = \frac{\max\{|s(n)|^2, n = 0, \frac{1}{V}, \frac{2}{V}, ..., N_c - 1\}}{E[|s(n)|^2]}, \quad (5)$$

where V represents oversampling factor. In case of multi-antenna transmission, the PAPR is averaged and calculated from the transmit signal from each transmit antenna.

The phase rotation patterns $\mathbf{P}_u = diag[P_u(0), \ldots, P_u(N_c-1)]$, $u=0 \sim U-1$ are defined in a random approach, i.e. $P_u(k) = \pm 1$, $k=0 \sim N_c-1$, except the first rotation pattern is an identity matrix $\mathbf{I}_{N_c}$. The binary random phase rotation patterns are selected in this paper since it achieves the lowest PAPR among various sequences without the requirement of additional complex-valued multiplication [13]. Time-domain transmit block candidates regarding to $\mathbf{P}_u$ at the q-th block and the n_t-th antenna are defined as $\tilde{\mathbf{s}}_{u,q,n_t} = \mathbf{F}_{N_c}^H \mathbf{H}_T \mathbf{P}_u \mathbf{S}_{q,n_t}$. The instantaneous PAPR of $\tilde{\mathbf{s}}_{u,q,n_t}$ is calculated for all $q=0 \sim Q-1$ and $n_t=0 \sim N_t-1$ by referencing (4), where its oversampled version is obtained by padding $(V-1)N_c$ zeros to $\mathbf{H}_T \mathbf{P}_u \mathbf{S}_{q,n_t}$ and then applying VN_c-point IDFT.

The common phase rotation pattern $\mathbf{P}_{\hat{u}}$ is selected in order to minimize the maximum value of PAPR among transmit blocks and transmit antennas $\tilde{\mathbf{s}}_{u,q,n_t}$ for all $u=0 \sim U-1$, $q=0 \sim Q-1$ and $n_t=0 \sim N_t-1$ (i.e. Mini-max criterion), that is

$$\mathbf{P}_{\hat{u}} = \arg \min_{u=0,1,\ldots,U-1} (\max(\mathrm{PAPR}(\tilde{\mathbf{s}}_{u,q,n_t} = \mathbf{F}_{N_c}^H \mathbf{H}_T \mathbf{P}_u \mathbf{S}_{q,n_t}))). \quad (6)$$

The searching criterion in (6) requires $U \times Q \times N_c$ computation times. We can further reduce the computation times by utilizing the characteristic of the STBC encoder in (2) that the output signal after STBC encoding $\mathbf{S}_{q,n_t}$ are either the original or the complex-conjugate of $\mathbf{D}_j$, and the fact that $\mathrm{PAPR}(\mathbf{F}_{N_c}^H \mathbf{D}_j^*) = \mathrm{PAPR}(\mathbf{F}_{N_c}^H \mathbf{D}_j)$. Therefore, (6) can be rewritten as

$$\mathbf{P}_{\hat{u}} = \arg \min_{u=0,1,\ldots,U-1} (\max(\mathrm{PAPR}(\tilde{\mathbf{s}}_{u,j} = \mathbf{F}_{N_c}^H \mathbf{H}_T \mathbf{P}_u \mathbf{D}_j))), \quad (7)$$

in which the computation times can be reduced from $U \times Q \times N_c$ to be $U \times J$.

3. Receiver with joint blind phase rotation pattern estimation & data detection

The STBC-SC-FDE receiver equipped with joint blind phase rotation pattern estimation & data detection is illustrated by Fig. 2. It can be seen that the receiver consists of two main processes; joint FDE based on minimum mean-square error (MMSE-FDE) and STBC decoding, and joint blind phase rotation pattern estimation & data detection, which are described in Subsection 3.1 and 3.2, respectively.

3.1. Joint MMSE-FDE and STBC decoding

The wireless propagation channel is assumed to be a symbol-spaced L-path frequency-selective block Rayleigh fading channel [3], where its impulse response between the transmit antenna n_t and received antenna n_r is given by

$$h_{n_r,n_t}(\tau) = \sum_{l=0}^{L-1} h_{n_r,n_t,l} \delta(\tau - \tau_{n_r,n_t,l}), \quad (8)$$

where $h_{n_r,n_t,l}$ and $\tau_{n_r,n_t,l}$ are complex-valued path gain and time delay of the l-th path, respectively. In addition, $h_{n_r,n_t,l}$ is assumed to be the same for Q encoded block in this paper for simplicity.

The q-th block discrete-time received signal at the n_r-th distributed antenna $\mathbf{r}_{q,n_r} = [r_{q,n_r}(0), r_{q,n_r}(1), ..., r_{q,n_r}(N_c-1)]^T$ can be expressed by

$$r_{q,n_r}(n) = \sqrt{\frac{2E_s}{T_s}} \sum_{n_t=0}^{N_t-1} \sum_{l=0}^{L-1} h_{n_r,n_t,l} \tilde{s}_{\hat{u},q,n_t}(n - \tau_{n_r,n_t,l}) + z_{q,n_r}(n), \quad (9)$$

where $z_{q,n_r}(n)$ is an additive white Gaussian noise (AWGN) having zero mean and the variance of $2N_0/T_s$ with T_s is symbol duration and N_0 being the one-sided noise power spectrum density. Note that the path-loss and shadowing-loss of transmission links between transmitter and distributed antennas are neglected. After CP removal, $r_{q,n_r}(n)$ is transformed into frequency domain by N_c-point DFT, yielding the frequency-domain received signal vector $\mathbf{R}_{q,n_r} = [R_{q,n_r}(0), R_{q,n_r}(1), ..., R_{q,n_r}(N_c-1)]^T$ as

$$R_{q,n_r}(k) = \sqrt{\frac{2E_s}{T_s}} \sum_{n_t=0}^{N_t-1} H_{n_r,n_t}(k) \tilde{S}_{\hat{u},q,n_t}(k) + Z_{q,n_r}(k), \quad (10)$$

where $\tilde{S}_{\hat{u},q,n_t}(k)$ is an element at the k-th frequency index of $\tilde{\mathbf{S}}_{\hat{u},q,n_t}$ in (3). The frequency-domain channel response and noise are expressed by

$$H_{n_r,n_t}(k) = \sum_{l=0}^{L-1} h_{n_r,n_t,l} \exp(-j2\pi k \tau_{n_r,n_t,l} / N_c), \quad (11a)$$

$$Z_{q,n_r}(k) = \frac{1}{N_c} \sum_{n=0}^{N_c-1} z_{q,n_r}(n) \exp(-j2\pi k n / N_c). \quad (11b)$$

FDE based on minimum mean-square error criterion (MMSE-FDE) is conducted by multiplying the MMSE weight matrix to the frequency-domain received matrix, then obtaining the equalized signal as $\tilde{\mathbf{R}}_{(N_t \times Q)} = \mathbf{W}_{(N_t \times N_r)}^H \mathbf{R}_{(N_r \times Q)}$, where $\mathbf{W} = [\mathbf{W}_0, ..., \mathbf{W}_{n_r}, ..., \mathbf{W}_{N_r-1}]$ and $\mathbf{W}_{n_r} = [\mathbf{W}_{n_r,0}, ..., \mathbf{W}_{n_r,n_t}, ..., \mathbf{W}_{n_r,N_t-1}]^T$ represents the MMSE-FDE weight matrix. The FDE weight at the k-th frequency index is expressed by [9-10].

$$W_{n_r,n_t}(k) = \frac{H_{n_r,n_t}(k)}{(\sum_{n_r=0}^{N_r-1} \sum_{n_t=0}^{N_t-1} |H_{n_r,n_t}(k)|^2) / N_t + (E_s / N_0)^{-1}}. \quad (12)$$

After that, STBC decoding is carried out in order to achieve diversity gain. The frequency-domain decoded vector $\hat{\mathbf{D}}_j$, $j=0 \sim J-1$ is obtained by the following STBC decoders [11], which employ only addition, subtraction and complex-conjugate operations on $\tilde{\mathbf{R}}_{q,n_t}$ where $\tilde{\mathbf{R}}_{q,n_t}$ is the matrix element in $\tilde{\mathbf{R}}$:

$$\hat{\mathbf{D}}_{N_t=1} = \tilde{\mathbf{R}}_{0,0}, \tag{13a}$$

$$\hat{\mathbf{D}}_{N_t=2} = \begin{bmatrix} \hat{\mathbf{D}}_0 \\ \hat{\mathbf{D}}_1 \end{bmatrix} = \begin{bmatrix} \tilde{\mathbf{R}}_{0,0} + \tilde{\mathbf{R}}^*_{1,1} \\ \tilde{\mathbf{R}}_{0,1} - \tilde{\mathbf{R}}^*_{1,0} \end{bmatrix}, \tag{13b}$$

$$\hat{\mathbf{D}}_{N_t=3} = \begin{bmatrix} \hat{\mathbf{D}}_0 \\ \hat{\mathbf{D}}_1 \\ \hat{\mathbf{D}}_2 \end{bmatrix} = \begin{bmatrix} \tilde{\mathbf{R}}_{0,0} + \tilde{\mathbf{R}}^*_{1,1} + \tilde{\mathbf{R}}^*_{2,2} \\ \tilde{\mathbf{R}}_{0,1} - \tilde{\mathbf{R}}^*_{1,0} + \tilde{\mathbf{R}}^*_{3,2} \\ \tilde{\mathbf{R}}_{0,2} - \tilde{\mathbf{R}}^*_{2,0} - \tilde{\mathbf{R}}^*_{3,1} \end{bmatrix}, \tag{13c}$$

$$\hat{\mathbf{D}}_{N_t=4} = \begin{bmatrix} \hat{\mathbf{D}}_0 \\ \hat{\mathbf{D}}_1 \\ \hat{\mathbf{D}}_2 \end{bmatrix} = \begin{bmatrix} \tilde{\mathbf{R}}_{0,0} + \tilde{\mathbf{R}}^*_{1,1} + \tilde{\mathbf{R}}^*_{2,2} + \tilde{\mathbf{R}}_{3,3} \\ \tilde{\mathbf{R}}_{0,1} - \tilde{\mathbf{R}}^*_{1,0} - \tilde{\mathbf{R}}_{2,3} + \tilde{\mathbf{R}}^*_{3,2} \\ \tilde{\mathbf{R}}_{0,2} + \tilde{\mathbf{R}}_{1,3} - \tilde{\mathbf{R}}^*_{2,0} - \tilde{\mathbf{R}}^*_{3,1} \end{bmatrix}. \tag{13d}$$

Note that the STBC decoding in (13) can be carried out without any modifications since the use of common phase rotation pattern can preserve the STBC code orthogonality, in other words, the conventional STBC decoding can remove the inter-antenna interference (IAI) even though $\tilde{\mathbf{R}}_{q,n_r}$ remains phase-rotated.

3.2. Blind phase rotation pattern estimation & data detection

In the conventional transmission using SLM techniques, the received signal vector after STBC decoding $\hat{\mathbf{D}}_j$, j=0~J–1 is typically de-mapped (i.e. phase rotation removal) by multiplying $\mathbf{P}^H_{\hat{u}}$, then obtaining time-domain received vector before data de-modulation $\hat{\mathbf{d}}_j = [\hat{d}_j(0),...,\hat{d}_j(N_c-1)]^T$, j=0~J–1 as $\hat{\mathbf{d}}_j = \mathbf{F}^H_{N_c}\mathbf{P}^H_{\hat{u}}\hat{\mathbf{D}}_j$. However, the above data detection technique requires side-information sharing, which degrades the spectrum efficiency.

We alternatively employ the joint blind phase rotation pattern estimation and data detection [8] in the receiver, which is expected to detect the signal effectively under an absence of side-information. The joint blind phase rotation pattern estimation and data detection is carried out by firstly generating all possible time-domain received vector candidates of the j-th block regarding to all U phase rotation patterns as

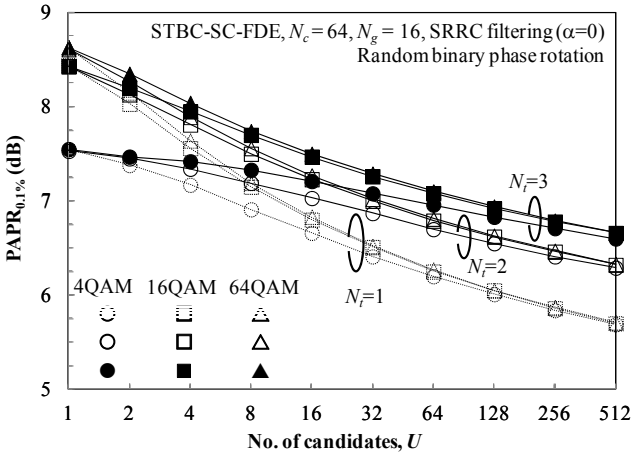

Fig.3 PAPR0.1% versus the number of candidates.

$$\mathbf{r}^{demap}_{j,v} = \mathbf{F}^H_{N_c}\mathbf{P}^H_v\hat{\mathbf{D}}_j, \tag{14}$$

where j=0~J–1 and v=0~U–1.

To decide which received vector candidate is likely to be the correct received vector, we utilize the fact that the received vector with correct de-mapping, i.e. $\mathbf{r}^{demap}_{j,v} = \mathbf{F}^H_{N_c}\mathbf{P}^H_v\hat{\mathbf{D}}_j$ where $v=\hat{u}$, and the received vector with incorrect de-mapping, i.e. $\mathbf{r}^{demap}_{j,v} = \mathbf{F}^H_{N_c}\mathbf{P}^H_v\hat{\mathbf{D}}_j$ where $v\neq\hat{u}$, are different and noticeable [8]. The received signal vector $\mathbf{r}^{demap}_{j,v} = \mathbf{F}^H_{N_c}\mathbf{P}^H_v\hat{\mathbf{D}}_j$ where $v=\hat{u}$ assuming high signal-to-noise power ratio (SNR) becomes concentrated at the original signal constellations. On the other hand, the received signal samples become dispersive when $v\neq\hat{u}$.

The difference between signals with correct and incorrect de-mapping can be differentiated by calculating the MSE, which is similar to the maximum-likelihood (ML) signal detection [14]. The ML-based signal detection can be expressed by

$$\hat{\mathbf{d}}_j = \min_{\substack{v=0,1,...,U-1, \\ \hat{d}_j(n)\in\Psi_{\mathrm{mod}}}} \frac{1}{N_c}\sum_{n=0}^{N_c-1}\left|r^{demap}_{j,v}(n) - \hat{d}_j(n)\right|^2, \tag{15}$$

where $\mathbf{r}^{demap}_{j,v}$ is defined in (14) and Ψ_{mod} is a set of original signal constellations for each modulation level. Note that (15) is applicable when the set of phase rotation patterns $\mathbf{P}_u$=*diag*[$P_u(0),...,P_u(N_c-1)$], u=0~U–1 is fixed and is known *a priori* at the receiver. Note that the selected phase rotation pattern is also estimated simultaneously with data detection, but the information of phase rotation pattern is not used.

Table 2 Simulation parameters.

Transmitter	Data modulation	4QAM, 16QAM, 64QAM
	No. of subcarriers	N_c = 64
	CP length	N_g = 16
	Transmit filtering	SRRC (α = 0)
SLM parameters	SLM algorithm	FD-SLM
	Phase-rotation sequence type	Random binary (1, -1)
	# of candidates	U = 1(no SLM)~512
	Oversampling factor	V = 8
Channel	Fading	Frequency-selective block Rayleigh
	Power delay profile	Symbol-spaced, 16-path uniform
Receiver	Channel estimation	Ideal
	Side-information	Ideal detection
	FDE	Received MMSE-FDE

4. Performance Evaluation

Numerical and simulation parameters are summarized in Table 2. We assume 4QAM, 16QAM and 64QAM block transmission with the number of available subcarriers N_c=64. Channel coding is not considered. Channel estimation and side-information detection (in case of FD-SLM with side-information sharing) are assumed to be ideal. A set of phase rotation patterns is generated in

random approach from binary phase rotation (1, -1), however, the set is used for all transmit blocks and is shared as a codebook between transceiver. The above phase rotation pattern sharing technique is also used in case of transmission with side-information sharing where the required side-information bits are $\log_2 U$ [6,14]. Performance of STBC-SC-FDE using the proposed FD-SLM and joint blind phase rotation pattern estimation and data detection (hereinafter called blind FD-SLM) is evaluated in terms of PAPR and BER, and then is compared to the conventional transmission techniques.

4.1. $PAPR_{0.1\%}$

PAPR performance is evaluated by measuring the PAPR value at complementary cumulative distribution function (CCDF) equals 10^{-3}, called $PAPR_{0.1\%}$, where its definition is $prob(\text{PAPR}(\mathbf{s}) \geq \text{PAPR}_{0.1\%}) = 10^{-3}$.

Fig. 3 shows the $PAPR_{0.1\%}$ of STBC-SC-FDE using the proposed blind FD-SLM compared to the conventional STBC-SC-FDE and single-antenna SC-FDE using FD-SLM [8]. It is obviously seen that PAPR reduces when the number of candidates U increases for all modulation schemes. This is consistent with the results in [7-8] as increasing U leads to an increasing of degree of freedom in candidate generation, and consequently increasing the probability of getting low-PAPR candidates.

It is also seen from Fig. 3 that the $PAPR_{0.1\%}$ increases when the number of transmit antennas N_t increases, in particular, $PAPR_{0.1\%}$ increases up to 0.5 dB of when N_t increases from 1 to 2. This is because the mini-max criterion in (7) decreases the degree of freedom and hence cannot guarantee an optimal solution for every transmission block. However, it was mentioned in Section 1 and 3 that the proposed FD-SLM using common phase rotation pattern remains attractive since it preserves the STBC code orthogonality and allows signal detection without side-information sharing.

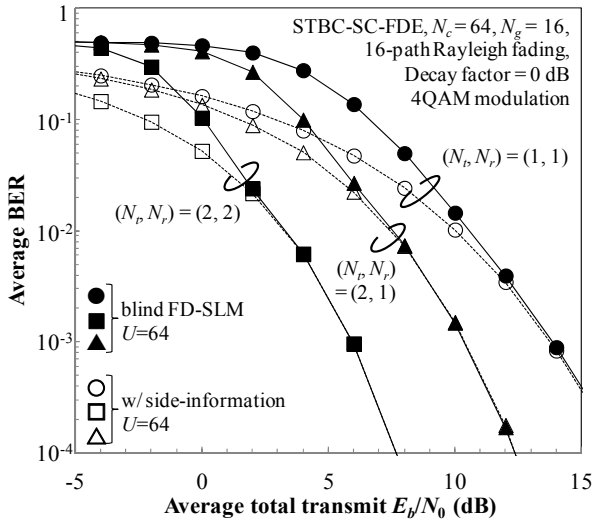

(a) 2 transmit antennas

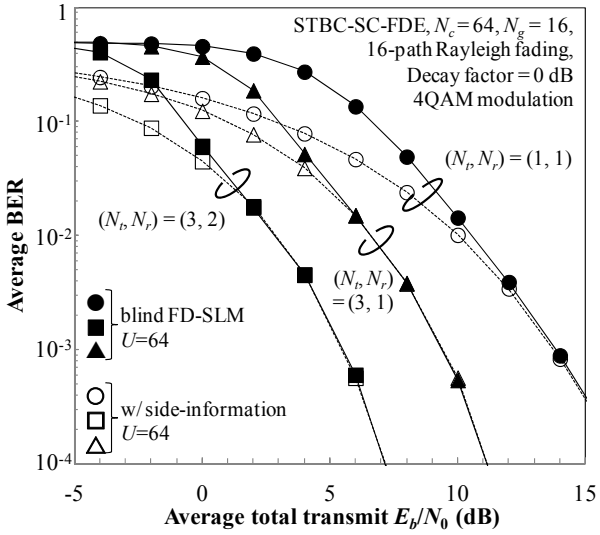

(b) 3 transmit antennas

Fig.4 BER performances.

4.2. BER performance

Fig. 4(a) and 4(b) show the BER performances of the proposed STBC-SC-FDE using the proposed blind FD-SLM as a function of average total transmit bit energy-to-noise power spectrum density ratio $E_b/N_0 = (1/N_{\text{mod}})(E_s/N_0)(1+N_g/N_c)$ where N_{mod} represents modulation level (2 for 4QAM, 4 for 16QAM and 6 for 64QAM) assuming N_t=2 and 3, respectively. BER performances of transmission using FD-SLM with ideal side-information sharing are also plotted for comparison. The number of candidates is assumed to be U=64.

It is obviously seen from Fig. 4(a) and 4(b) that the BER improves in both the transmission using FD-SLM with side-information sharing and blind FD-SLM when either N_t or N_r increases because of an increasing of STBC diversity gain. The BER performance of STBC-SC-FDE using blind FD-SLM degrades compared to that of FD-SLM with ideal side-information sharing when the transmit power is low. This result is also consistent with [8] assuming N_t=1 since the effect from noise power and residual ISI makes the time-domain received signal vector becomes dispersive even though the de-mapping is carried out correctly. However, there is no difference on BER performances of STBC-SC-FDE using the proposed blind FD-SLM and that of STBC-SC-FDE using FD-SLM with ideal side-information sharing when the transmit power is high, especially at the place that BER is less than 0.01.

5. Conclusion

The PAPR reduction in SC-FDE transmission is still am important issue for the uplink signal transmission even in 5G small-cell network using distributed antennas. In this paper, a new blind FD-SLM was proposed for the uplink transmission using STBC-SC-FDE. The proposed blind FD-SLM applies a common phase rotation pattern to all transmit antennas, where the pattern is selected so as to

minimize the maximum PAPR among all transmit signals from user terminal antennas. Advantage of the joint blind phase rotation pattern estimation and data detection is that the STBC decoding can be carried out without side-information sharing. Computer simulation results confirmed that without significant BER degradation, the proposed blind FD-SLM achieves a low PAPR close to the individual FD-SLM.

Acknowledgement

This research was funded by the national project of "Research and Development on 5G mobile communications system" (#0155-0171, Sept. 2015), supported by the Ministry of Internal Affairs and Communications (MIC), Japan.

References

[1] F. Adachi, K. Takeda, T. Yamamoto, R. Matsukawa and S. Kumagai, "Recent Advances in Single-Carrier Distributed Antenna Network," *Wiley Wireless Commun. and Moblie Comput.*, Vol. 11, pp. 1551-1563, Dec. 2011.

[2] D. Falconer, S. L. Ariyavisitakul, A. Benyamin-Seeyar and B. Edison, "Frequency Domain Equalization for Single-Carrier Broadband Wireless Systems," *IEEE Commun. Mag.*, Vol. 40, No. 4, pp. 58-66, Apr. 2002.

[3] A. Goldsmith, *Wireless Communications*, Cambridge University Press, 2005.

[4] H. Sari, G. Karam and I. Jeanclaude, "Transmission Techniques for Digital Terrestrial TV Broadcasting," *IEEE Commun. Mag.*, Vol. 33, No. 2, pp. 100-109, Feb. 1995.

[5] A. Boonkajay, T. Obara, T. Yamamoto and F. Adachi, "Excess-Bandwidth Transmit Filtering Based on Minimization of Variance of Instantaneous Transmit Power for Low-PAPR SC-FDE," *IEICE Trans. Commun.*, Vol. E98-B, No. 4, pp. 673-685, Apr. 2015.

[6] R. W. Bauml, R. F. H. Fischer and J. B. Huber, "Reducing the Peak-to-Average Power Ratio of Multicarrier Modulation by Selected Mapping," *IEEE Electron. Lett.*, Vol. 32, No. 22, pp. 2056-2057, Oct. 1996.

[7] A. Boonkajay, T. Obara, T. Yamamoto and F. Adachi, "Selective Mapping for Broadband Single-Carrier Transmission Using Joint Tx/Rx MMSE-FDE," *in Proc. IEEE Int. Symp. On Personal Indoor and Mobile Radio Commun. (PIMRC2013)*, London, U.K., Sept. 2013.

[8] A. Boonkajay and F. Adachi, "A Blind Selected Mapping Technique for Low-PAPR Single-Carrier Signal Transmission," *to be presented in Int. Conference on Inform. Commun. and Signal Process. (ICICS2015)*, Singapore, Dec. 2015.

[9] J. R. Hampton, *Introduction to MIMO Communications*, Cambridge University Press, 2013.

[10] S. M. Alamouti, "A simple transmit diversity technique for wireless communications," *IEEE J. Select. Areas. Commun.*, Vol. 16, No. 8, pp. 1451-1458, Oct. 1998.

[11] V. Tarokh, H. Jafarkhani, and A. R. Calderbank, "Space-time block coding for wireless communications: performance results," *IEEE J. Select. Areas. Commun.*, Vol. 17, No. 3, pp. 451-460, Mar. 1999.

[12] G. Ganesan and P. Stoica, "Space-time block codes: A maximum SNR approach," *IEEE Trans. Inform. Theory*, Vol. 48, No. 2, pp. 1650–1656, Apr. 2001.

[13] G. T. Zhou and L. Peng, "Optimality Condition for Selected Mapping in OFDM," *IEEE Trans. Signal Process.*, Vol. 54, No. 8, pp. 3159-3165, Aug. 2006.

[14] J. G. Proakis and M. Salehi, *Digital Communications*, 5th ed., McGraw-Hill, 2008.